nature materials

LETTERS

PUBLISHED ONLINE: 29 NOVEMBER 2009 | DOI: 10.1038/NMAT2588

Highly efficient photocathodes for dye-sensitized tandem solar cells

A. Nattestad[1], A. J. Mozer[2], M. K. R. Fischer[3], Y.-B. Cheng[1], A. Mishra[3], P. Bäuerle[3]*† and U. Bach[1,4]*†

Thin-film dye-sensitized solar cells (DSCs) based on mesoporous semiconductor electrodes are low-cost alternatives to conventional silicon devices[1,2]. High-efficiency DSCs typically operate as photoanodes (n-DSCs), where photocurrents result from dye-sensitized electron injection into n-type semiconductors. Dye-sensitized photocathodes (p-DSCs) operate in an inverse mode, where dye-excitation is followed by rapid electron transfer from a p-type semiconductor to the dye (dye-sensitized hole injection). Such p-DSCs and n-DSCs can be combined to construct tandem solar cells[3] (pn-DSCs) with a theoretical efficiency limitation well beyond that of single-junction DSCs (ref. 4). Nevertheless, the efficiencies of such tandem pn-DSCs have so far been hampered by the poor performance of the available p-DSCs (refs 3, 5–15). Here we show for the first time that p-DSCs can convert absorbed photons to electrons with yields of up to 96%, resulting in a sevenfold increase in energy conversion efficiency compared with previously reported photocathodes[7]. The donor–acceptor dyes, studied as photocathodic sensitizers, comprise a variable-length oligothiophene bridge, which provides control over the spatial separation of the photogenerated charge carriers. As a result, charge recombination is decelerated by several orders of magnitude and tandem pn-DSCs can be constructed that exceed the efficiency of their individual components.

Photocurrent matching is an essential prerequisite for the realization of highly efficient tandem pn-DSCs. The poor photovoltaic performance of p-DSCs reported until now has so far prohibited the fabrication of high-efficiency tandem pn-DSCs and raised questions concerning the fundamental efficiency limitations for photocathodic solar cells. Fast charge recombination following dye-sensitized hole injection generally resulted in low photocurrents. Here we studied a series of donor–acceptor dyes to elucidate the main factor that determines charge recombination dynamics and thereby the photovoltaic performance of dye-sensitized NiO solar cells.

The chemical structures of three donor–acceptor-type dyes **1**–**3**, comprising a perylenemonoimid (PMI) as the acceptor and an oligothiophene coupled to triphenylamine as the donor are shown in Fig. 1a. The length of the regioregularly alkylated oligo-3-hexylthiophene unit was systematically varied from a bithiophene ($n=1$; **1**) to a quaterthiophene ($n=2$; **2**) and a sexithiophene ($n=3$; **3**). In contrast to donor–acceptor-type dyes used in conventional TiO_2 photoanodes, here, the carboxylic acid anchoring groups are attached to the donor component. This has recently been reported to be an important design feature for efficient NiO photocathode sensitizers[9,11]. Figure 1b reveals that the electron density of the lowest unoccupied molecular orbital (LUMO) for dyes **1**–**3** is located exclusively at the PMI and the adjacent thiophene ring, whereas that of the highest occupied molecular orbital (HOMO) is distributed more evenly over the entire π-conjugated system. The initial charge-separation step in photocathodes involves the transfer of an electron from the valence band of the NiO to the HOMO of the dye, following its electronic excitation. Alternatively, this process can be described as dye-sensitized hole injection into the p-type material (Supplementary Fig. S1).

Figure 2a shows the transient absorption spectrum of a mesoporous NiO film, sensitized with dye **3**, after laser excitation. The spectrum features a typical dye-bleaching signal at wavelengths shorter than 550 nm and a positive transient-absorption feature at higher wavelengths, characteristic for the absorption profile of the reduced dye[16,17]. The latter suggests that the observed absorption changes are due to the formation of reduced **3**. The inset of Fig. 2 shows the kinetic traces recorded for dyes **1**–**3** at an observation wavelength of 700 nm. The observable signal decay reflects the recombination dynamics of the photoreduced dyes with vacancies present in the valence band of the NiO. The signal rise times were within the laser pulse duration (<10 ns), consistent with previous observations of sub-nanosecond dye-sensitized hole injection into the valence band of NiO (refs 5, 8, 9, 13). The kinetic traces were fitted to a double exponential decay, yielding t_1(t_2) recombination time constants of 0.17 μs (1.34 μs), 1.22 μs (12.17 μs) and 2.54 μs (13.56 μs) for sensitizers **1**–**3**, respectively. This shows a clear correlation between the length of the oligothiophene linker and the observed recombination kinetics. Dye **3** shows recombination kinetics that are several orders of magnitude slower than the slowest recombination process reported so far for dye-sensitized NiO (ref. 9).

Previous surface adsorption studies of **1** revealed a Langmuir-type adsorption behaviour ($\Gamma_0 = 1.46 \pm 0.05\ \mu mol\ m^{-2}$), suggesting that the long axis of the molecule is aligned predominantly perpendicular to the metal oxide surface, facilitated through the binding of the carboxylic acid groups[16]. Assuming a similar molecular orientation of compounds **1**–**3** on their adsorption on NiO, an increasing length of the oligothiophene bridge translates into an increased tunnelling distance between the electron occupying the dye's LUMO shown in Fig. 1b and the vacancies located in the NiO electrode. Calculating the distance between the centres of the thiophene unit attached to the PMI and the closest carboxyl oxygen yields estimates for the tunnelling distances of 1.3, 2.1 and 2.8 nm for dyes **1**, **2** and **3**, respectively.

[1]ARC Centre of Excellence for Electromaterials Science, Department of Materials Engineering, Monash University, Clayton Victoria, 3800, Australia, [2]ARC Centre of Excellence for Electromaterials Science, Intelligent Polymer Research Institute, AIIM Facility, Innovation Campus, University of Wollongong, New South Wales, 2522, Australia, [3]Institute for Organic Chemistry II and Advanced Materials, University of Ulm, Albert-Einstein-Allee 11, 89081 Ulm, Germany, [4]ARC Centre of Excellence for Electromaterials Science, School of Chemistry, Monash University, Clayton Victoria, 3800, Australia. *These authors contributed equally to this work. †e-mail: peter.baeuerle@uni-ulm.de; udo.bach@sci.monash.edu.au.

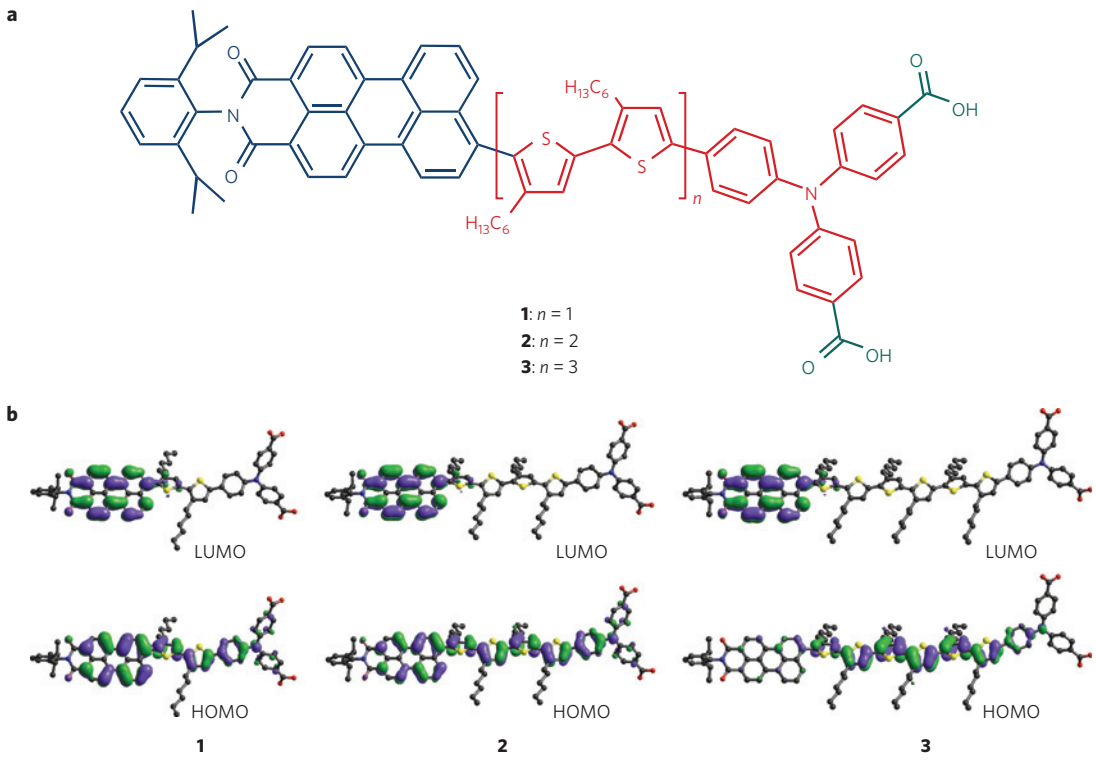

Figure 1 | NiO photocathode sensitizers. a, Chemical structure of donor–acceptor dyes **1**–**3**. **b**, Electron-density distribution for the LUMOs and HOMOs of dyes **1**–**3**. The quantum-chemical Austin Model 1 method under restricted Hartree–Fock conditions was used to analyse the electron distribution in the frontier orbitals of these dyes.

Electron-transfer rates can also be affected by the energetic position of the dye's LUMO. However, cyclovoltammetric analysis of dyes **1**–**3** showed variations in the reduction potentials of less than 20 mV (refs 16, 17). These small differences are unlikely to cause the significant changes in electron-transfer rates observed for this dye series. Efficient lateral electron transfer between adjunct PMI units, as previously observed in self-assembled monolayers of **1** on different metal oxide substrates, could further contribute to the retarded charge recombination observed in these systems[16]. In conclusion, it is possible to gain excellent control over the prevailing recombination phenomena in dye-sensitized NiO by tailoring the distance between the acceptor functionality and the attachment group of the sensitizer. Increased tunnelling distances for charge recombination with increased length of the oligothiophene linker therefore appears to be the predominant mechanism responsible for the observed retardation of recombination.

Figure 3 shows the incident photon-to-electron conversion efficiency (IPCE) spectra of typical p-DSCs based on mesoporous NiO electrodes sensitized with dyes **1**–**3**. The light-harvesting efficiency of the dye layers adsorbed onto the 1.25-μm-thick NiO were measured and are shown for comparison (see also Supplementary Information, S2). The shapes of the IPCE spectra closely match the optical absorptivity of the corresponding dyes, confirming that the observed photocurrents are dye-sensitized. A comparison of the IPCE and absorptivity curves also reveals a pronounced variation in the absorbed photon-to-electron conversion efficiency (APCE), defined as the ratio of IPCE to absorptivity. The APCE values, averaged over the spectral range 400–500 nm for dyes **1**–**3** were 28%, 53% and 96%, respectively (Supplementary Information, S2). This clearly shows that the lower IPCE values observed for dyes **1** and **2** do not originate from inferior light-harvesting efficiencies. The highest APCE value reported so far for dye-sensitized NiO p-DSCs is 45%, calculated for a device with a maximum IPCE of 4% (ref. 9). Low APCE values can either be a result of inefficient hole injection or the loss of initially formed charge carriers through recombination. Transient laser spectroscopy here clearly revealed that charge recombination rates decrease with increasing length of the oligothiophene bridge. At the same time, the initial amplitude of the transient absorption signal normalized to the absorbed pump intensity is comparable for all three dyes (Supplementary Information, S1), indicating only minor differences in the charge generation yield ~100 ns after laser excitation. This indicates similar charge-injection efficiencies for dyes **1**–**3**. The results show that the increase in efficiency with increasing length of the oligothiophene bridge results primarily from reduced charge recombination on the recorded 100 ns–100 μs timescale. The increased hydrophobicity of the dyes with increasing length of the oligothiophene linker could also help to shield the NiO surface from the electrolyte. Similar effects have previously been observed for ruthenium complexes carrying hydrophobic substituents that showed delayed interfacial charge recombination in n-DSCs (ref. 18).

Figure 3 also shows the IPCE spectrum of a typical p-DSC assembled from a 2.3-μm-thick NiO film sensitized with dye **3**. The peak IPCE value of 62% is a factor of three greater than any previously reported IPCE for p-DSCs observed at the longest wavelength absorption band of a sensitizer[10]. A further increase in the NiO layer thickness did not result in any improvement of the IPCE values. This can be rationalized in terms of the absorptivity of the NiO film that absorbs 30–40% of the incident photons over most of the visible wavelength range. Photons absorbed by the NiO do not yield any observable photocurrents.

Figure 4b shows the typical current–voltage curves of p-DSCs sensitized with dyes **1**–**3**. Short-circuit current densities (J_{SC}), fill factors, open-circuit voltages (V_{OC}) as well as the overall energy-conversion efficiency (η) drastically increase with increasing length of the oligothiophene linker in dyes **1**–**3**. The values of J_{SC} (5.35 mA cm^{-2}) and V_{OC} (218 mV) obtained for dye **3** are

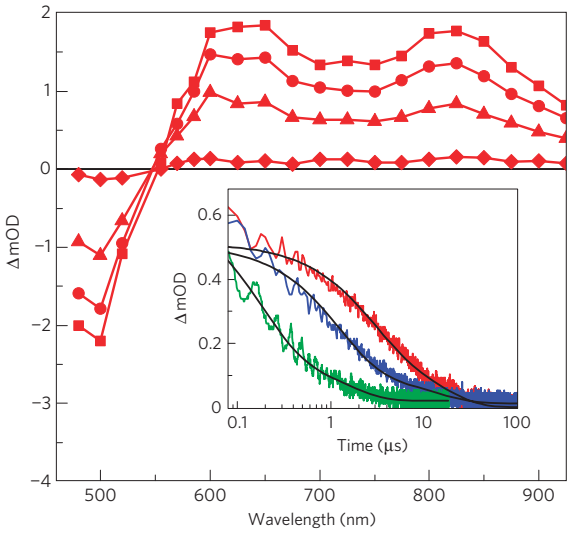

Figure 2 | Transient absorption spectroscopy and recombination dynamics. The transient absorption spectrum of mesoporous NiO films, sensitized with dye **3**. The spectra were recorded 0.1 μs (squares), 0.3 μs (circles), 1.0 μs (triangles) and 10 μs (diamonds) after laser excitation at a wavelength of 532 nm with an average laser intensity of 220 μJ cm^{-2} per pulse. Inset: Transient absorption decay signals of NiO films sensitized with **1** (green), **2** (blue) and **3** (red). Observation wavelength: 700 nm, laser intensity 70 μJ cm^{-2} per pulse for **1** and **2** and 35 μJ cm^{-2} for **3**. The absorbance of the dye-sensitized films at 532 nm was 0.19, 0.22 and 0.34 for dye **1**, **2** and **3**, respectively (contact medium: glutaronitrile).

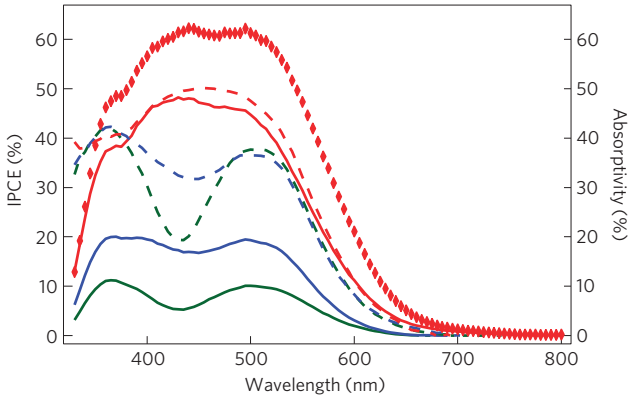

Figure 3 | IPCEs. The IPCE value corresponds to the number of electrons generated by monochromatic light in the external circuit, divided by the number of incident photons. IPCE spectra of p-DSCs assembled from mesoporous 1.25-μm-thick NiO electrodes (solid lines), sensitized with dyes **1** (green), **2** (blue) and **3** (red) as well as the percentage of incident photons that are absorbed by the dye inside the p-DSC (absorptivity, dashed lines). The red diamonds indicate the IPCE of a mesoporous 2.3-μm-thick NiO electrode sensitized with **3**. Platinum-coated conducting glass (fluorine-doped tin oxide) was used as a counter electrode.

unprecedented for p-DSCs and result in a sevenfold increase in energy-conversion efficiency compared with the most efficient p-DSC known so far[7].

A typical cross-section scheme of a pn-DSC with the approximate energy levels of each component is shown in Fig. 4a. The tandem cell consists of one photoanode and one photocathode in a simple sandwich configuration with an intermediate electrolyte layer. The series connection of photoanodes and photocathodes in tandem pn-DSCs implies that the resulting photocurrent will be governed by the weakest photoelectrode, whereas photovoltages are additive. Here, photocurrent matching was achieved through careful adjustment of NiO and TiO_2 film thicknesses to control the optical absorptions and hence match the respective photocurrents of both electrodes. Thickness requirements for optimized cell performances vary, depending on whether the device is illuminated through the sensitized NiO or TiO_2 side. Two tandem devices, optimized for illumination through either the photocathode or photoanode side were fabricated. Figure 4c shows the current–voltage characteristics of a tandem pn-DSC optimized for illumination through the photoanode (0.8 μm TiO_2; 3.3 μm NiO). For comparison, the performances of p-DSCs and n-DSCs assembled from the comprising electrodes are also shown. The tandem device features a photocurrent density similar to that of the n-DSC, whereas the open-circuit voltage (V_{OC}) of 1,079 mV closely matches the sum of V_{OC} for n-DSC and p-DSC. This results in a tandem solar cell that features an overall efficiency that clearly exceeds that of the comprising n-DSC. This is the first time that such an efficiency increase could be observed for the tandem pn-DSC concept studied here. The resulting open-circuit voltage of 1,079 mV is the highest ever reported for electrolyte-based photoelectrochemical solar cells. The improved fill factor of 74% for the tandem device is a further indication of successful current matching of p-DSC and n-DSC. Tandem pn-DSCs matched for illumination through the NiO electrode were also constructed (12 μm TiO_2; 1.55 μm NiO). The resulting tandem device showed higher efficiencies ($\eta = 2.42\%$) than the tandem pn-DSC presented in Fig. 4c, yet it was significantly less efficient than the equivalent n-DSC based on a 12 μm TiO_2 layer alone ($\eta = 5.9\%$; see Supplementary Fig. S2).

Although these record performances for tandem pn-DSCs are very encouraging, the overall device efficiencies are still considerably lower than those of high-performance n-DSCs. This can be mainly attributed to the very similar spectral response of **3** and N719 used as sensitizers, resulting in a situation where both sensitizers compete for photons in the same spectral range. Future efficient tandem DSCs will require the development of p-DSC sensitizers that are spectrally complementary to high-efficiency n-DSC sensitizers. Further efficiency increases can be achieved if alternative p-type semiconductors with a more favourable valence-band edge position become available, resulting in tandem cells with higher photovoltage.

In this work we show for the first time that dye-sensitized hole injection into p-type semiconductors and subsequent charge collection can proceed at quantum yields of almost unity. This is paving the way for the development of a new generation of highly efficient photocathodic p-DSCs with the scope to develop tandem pn-DSCs with efficiencies equal to or superior to conventional high-efficiency n-DSCs.

Alternative tandem DSC concepts have been reported in the past[19–22]. Most of these describe stacked device configurations of multiple fully pre-assembled DSCs (refs 19, 20) or the combination of DSCs with conventional Cu(In, Ga)Se_2 photovoltaic modules[21]. The advantage of the present approach lies in its potential to convert conventional DSCs into more efficient tandem DSCs with very minor changes, namely the replacement of the catalytic platinum layer with a dye-sensitized p-type semiconductor layer. This can be expected to involve only minor extra processing and material costs, making tandem pn-DSCs an economically viable option for the future.

Methods

Summary. Dye-sensitized p-DSCs, n-DSCs and tandem pn-DSCs were assembled as described elsewhere[3,14,23]. Mesoporous TiO_2 and NiO electrodes were printed using a commercial semiautomatic screen printer. Commercial TiO_2 screen-printing paste (PST-18NR, JGC Catalysts and Chemicals) was used as received. NiO screen-printing paste was produced by mixing a slurry of 15 g of NiO nanopowder (Inframat) in ethanol with 50 ml of 10 wt% ethanolic ethyl cellulose (Sigma Aldrich) solution and 100 ml terpineol, followed by slow ethanol

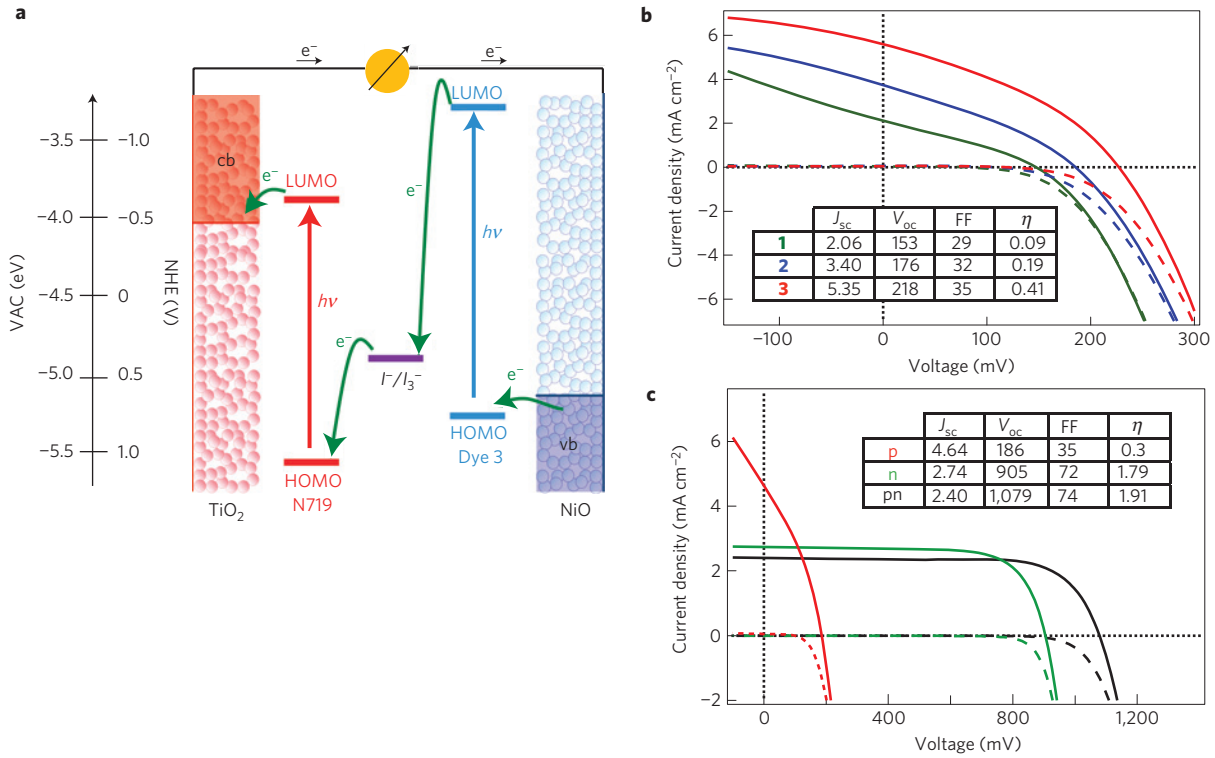

Figure 4 | Tandem cell structure and current-density–voltage characteristics. a, Scheme for the electron-transfer processes occurring in the dye-sensitized tandem solar cell. Also shown are the approximate redox potentials (versus normal hydrogen electrode, NHE) and band energies (versus vacuum level, VAC) of the different components. **b**, Current-density–voltage characteristics of the same devices as in Fig. 3 under simulated standard solar irradiation (AM1.5, 1,000 W m^{-2}, solid lines) and in the dark (dashed lines) for dyes **1**–**3**; green: **1**; blue: **2**; red: **3**. **c**, Current–voltage characteristics of a tandem solar cell (black) as well as p-DSCs (red) and n-DSCs (green) under illumination (AM1.5, 1,000W m^{-2}, solid lines) and in the dark (dashed lines). Identical NiO and TiO_2 films were used for the construction of the tandem, p- and n-DSC. The photocathodes consisted of a 3.3-μm-thick NiO layer sensitized with **3**. The photoanodes consisted of a 0.8-μm-thick TiO_2 layer, sensitized with $RuL_2(SCN)_2$(where L is tetrabutylammonium 4′-carboxy-2,2′-bipyridine-4-carboxylate, N719). The tandem pn-DSC and n-DSC were illuminated through the n-side; the p-DSC through the p-side. J_{SC}, short-circuit current density (mA cm^{-2}); V_{OC}, open-circuit voltage (mV); FF, fill factor (%); η, energy-conversion efficiency (%).

removal by rotary evaporation. NiO films were immersed in 0.1 mM solutions of **1**–**3** in dimethylformamide for 2 h for dye uptake. Electrolytes optimized for high-efficiency TiO_2 n-DSCs were used for all DSCs (0.6 M *N*-methyl-*N*-butyl imidazolium iodide, 0.5 M 4-*t*-butylpyridine, 0.1 M guanadinium thiocyanate and 30 mM iodine in 85:15 acetonitrile/valeronitrile). The I_2 concentration for devices described in Fig. 4c was adjusted to 15 mM. Compounds **1**–**3** were synthesized as described elsewhere[16,17]. Ru(II)$L_2(SCN)_2$ (N719, Dyesol) was used as received.

Photovoltaic characterization. A sun simulator (Oriel) fitted with a filtered 1,000 W xenon lamp was used to provide simulated air-mass 1.5 (AM1.5, 1,000 W m^{-2}) solar irradiation. Current–voltage curves were recorded using a Keithley 2400 source meter. The output of the light source was adjusted using a calibrated silicon photodiode (Peccell Technologies). The photodiode was fitted with a colour filter by the supplier, to minimize the optical mismatch between the calibration diode and the dye-sensitized solar cells. The spectral response (IPCE) was measured using a 150 W xenon lamp (Oriel) fitted with a monochromator (Cornerstone 260) as a monochromatic light source. The illumination spot size was chosen to be slightly smaller than the active area of the DSC test cells. IPCE photocurrents were recorded under short-circuit conditions using a Keithley 2400 source meter. The monochromatic photon flux was quantified by means of a calibrated silicon photodiode (Peccell Technologies).

Transient absorption spectroscopy. The second harmonic (532 nm) of a Q-switched Nd-YAG laser (INDI-40-10, Spectra-Physics) was used as a pump, producing 6-ns pulses of 10 Hz repetition rate. The intensity of the pump was attenuated using reflective filters to ~200 μJ cm^{-2} $pulse^{-1}$ to obtain the transient absorption spectrum and 70–35 μJ cm^{-2} $pulse^{-1}$ for the comparison of charge recombination kinetics. The light from a Xe lamp (Edinburgh Instruments) was spectrally narrowed by a combination of cutoff and band-pass filters (40 nm band pass) and focused on the sample. The transmitted light was refocused onto the slit of a monochromator and the changes in the transmission were detected by a 200 MHz amplified photodiode (Femto). A Tektronix 4054 oscilloscope with 20 MHz bandwidth was used to digitalize the traces. The kinetic traces shown in the inset of Fig. 2 were recorded at 700 nm and were fitted using a built-in double exponential function of Origin Pro 8.0. NiO films of 1.25 μm thickness were used for all transient absorption spectroscopy experiments.

Received 30 March 2009; accepted 26 October 2009; published online 29 November 2009

References

1. O'Regan, B. & Grätzel, M. A low-cost, high-efficiency solar-cell based on dye-sensitized colloidal TiO_2 films. *Nature* **353,** 737–740 (1991).
2. Grätzel, M. Photoelectrochemical cells. *Nature* **414,** 338–344 (2001).
3. He, J. J., Lindstrom, H., Hagfeldt, A. & Lindquist, S. E. Dye-sensitized nanostructured p-type nickel oxide film as a photocathode for a solar cell. *J. Phys. Chem. B* **103,** 8940–8943 (1999).
4. Henry, C. H. Limiting efficiencies of ideal single & multiple energy gap terrestrial solar cells. *J. Appl. Phys.* **51,** 4494–4500 (1980).
5. Borgstrom, M. *et al.* Sensitized hole injection of phosphorus porphyrin into NiO: Toward new photovoltaic devices. *J. Phys. Chem. B* **109,** 22928–22934 (2005).
6. He, J. J., Lindstrom, H., Hagfeldt, A. & Lindquist, S. E. Dye-sensitized nanostructured tandem cell-first demonstrated cell with a dye-sensitized photocathode. *Sol. Energy Mater. Sol. Cells* **62,** 265–273 (2000).
7. Mizoguchi, Y. & Fujihara, S. Fabrication and dye-sensitized solar cell performance of nanostructured NiO/Coumarin 343 photocathodes. *Electrochem. Solid State Lett.* **11,** K78–K80 (2008).
8. Morandeira, A., Boschloo, G., Hagfeldt, A. & Hammarstrom, L. Photoinduced ultrafast dynamics of coumarin 343 sensitized p-type-nanostructured NiO films. *J. Phys. Chem. B* **109,** 19403–19410 (2005).
9. Morandeira, A. *et al.* Improved photon-to-current conversion efficiency with a nanoporous p-type NiO electrode by the use of a sensitizer-acceptor dyad. *J. Phys. Chem. C* **112,** 1721–1728 (2008).
10. Mori, S. *et al.* Charge-transfer processes in dye-sensitized NiO solar cells. *J. Phys. Chem. C* **112,** 16134–16139 (2008).
11. Qin, P. *et al.* Design of an organic chromophore for p-type dye-sensitized solar cells. *J. Am. Chem. Soc.* **130,** 8570–8572 (2008).

12. Vera, F. *et al.* Preparation and characterization of Eosin B- and Erythrosin J-sensitized nanostructured NiO thin film photocathodes. *Thin Solid Films* **490,** 182–188 (2005).
13. Zhu, H., Hagfeldt, A. & Boschloo, G. Photoelectrochemistry of mesoporous NiO electrodes in iodide/triiodide electrolytes. *J. Phys. Chem. C* **111,** 17455–17458 (2007).
14. Nattestad, A., Ferguson, M., Kerr, R., Cheng, Y.-B. & Bach, U. Dye-sensitized nickel(II) oxide photocathodes for tandem solar cell applications. *Nanotechnology* **19,** 295304–295313 (2008).
15. Nakasa, A. *et al.* A high voltage dye-sensitized solar cell using a nanoporous NiO photocathode. *Chem. Lett.* **34,** 500–501 (2005).
16. Wang, Q. *et al.* Cross surface ambipolar charge percolation in molecular triads on mesoscopic oxide films. *J. Am. Chem. Soc.* **127,** 5706–5713 (2005).
17. Cremer, J. *Novel Head-to-Tail Coupled Oligo(3-Hexylthiophene) Derivatives for Photovoltaic Applications*. PhD thesis, Univ. Ulm (2005).
18. Zakeeruddin, S. M. *et al.* Design, synthesis, and application of amphiphilic ruthenium polypyridyl photosensitizers in solar cells based on nanocrystalline TiO_2 films. *Langmuir* **18,** 952–954 (2002).
19. Durr, M., Bamedi, A., Yasuda, A. & Nelles, G. Tandem dye-sensitized solar cell for improved power conversion efficiencies. *Appl. Phys. Lett.* **84,** 3397–3399 (2004).
20. Kubo, W., Sakamoto, A., Kitamura, T., Wada, Y. & Yanagida, S. Dye-sensitized solar cells: Improvement of spectral response by tandem structure. *J. Photochem. Photobiol. A: Chem.* **164,** 33–39 (2004).
21. Liska, P. *et al.* Nanocrystalline dye-sensitized solar cell/copper indium gallium selenide thin-film tandem showing greater than 15% conversion efficiency. *Appl. Phys. Lett.* **88,** 203103 (2006).
22. Murayama, M. & Mori, T. Dye-sensitized solar cell using novel tandem cell structure. *J. Phys. D* **40,** 1664–1668 (2007).
23. Ito, S. *et al.* Fabrication of thin film dye sensitised solar cells with a solar to electric power conversion efficiency over 10%. *Thin Solid Films* **516,** 4613–4619 (2008).

Acknowledgements

The authors would like to thank the Victorian Government (Department of Primary Industries, ETIS SERD), the ARC Centre of Excellence for Electromaterials Science (ACES), the German Academic Exchange Service (DAAD-Go8 joint research cooperation scheme) and the International Science Linkage Project CG 100059 (DIISR, Australia) for financial support. Furthermore, they would like to acknowledge the ARC for providing equipment support through LIEF, as well as supporting U.B. with an Australian Research Fellowship. Special thanks also to Monash University for supporting U.B. with a Monash Research Fellowship, as well as JGC Catalysts and Chemicals Ltd, Kitakyushu-Shi (Japan) for providing samples of TiO_2 screen-printing paste. We would like to thank the German Federal Ministry of Education and Research (BMBF) for financially supporting our research on organic solar-cell materials in the frame of a joint project (OPEG) and the Alexander von Humboldt Foundation for a grant for A.M. This work was also supported by the German Science Foundation (DFG) in the frame of a Collaborative Research Center (SFB 569). Finally we would also like to thank L. Kane-Maguire for assistance in the manuscript preparation process.

Author contributions

U.B. and P.B. proposed the research with further contributions from A.M. and Y.-B.C. A.N. carried out the photovoltaic characterization, optical analysis and optimized the tandem solar cells under the supervision of U.B. and Y.-B.C. Sensitizing dyes were designed and developed in the group of P.B. M.K.R.F. carried out the molecular orbital calculations. A.J.M. and U.B. executed the transient absorption spectroscopy measurements and interpreted the result. U.B., A.N., A.J.M. and M.K.R.F. were mainly responsible for writing the manuscript, with further inputs from P.B., Y.-B.C. and A.M.

Additional information

The authors declare no competing financial interests. Supplementary information accompanies this paper on www.nature.com/naturematerials. Reprints and permissions information is available online at http://npg.nature.com/reprintsandpermissions. Correspondence and requests for materials should be addressed to P.B. or U.B.